

Learning Collaborative Information Dissemination with Graph-based Multi-Agent Reinforcement Learning

Raffaele Galliera^{†,*}, Kristen Brent Venable^{†,*}, Matteo Bassani[†], Niranjan Suri^{†,*,‡}

[†]Institute for Human & Machine Cognition

^{*}Department of Intelligent Systems & Robotics, The University of West Florida

Pensacola, FL, USA

[‡]US Army Research Laboratory

Adelphi, MD, USA

{rgalliera, bvenable, mbassani, nsuri}@ihmc.org

Abstract

In modern communication systems, efficient and reliable information dissemination is crucial for supporting critical operations across domains like disaster response, autonomous vehicles, and sensor networks. This paper introduces a Multi-Agent Reinforcement Learning (MARL) approach as a significant step forward in achieving more decentralized, efficient, and collaborative solutions. We propose a Decentralized-POMDP formulation for information dissemination, empowering each agent to independently decide on message forwarding. This constitutes a significant paradigm shift from traditional heuristics based on Multi-Point Relay (MPR) selection. Our approach harnesses Graph Convolutional Reinforcement Learning, employing Graph Attention Networks (GAT) with dynamic attention to capture essential network features. We propose two approaches, L-DGN and HL-DGN, which differ in the information that is exchanged among agents. We evaluate the performance of our decentralized approaches, by comparing them with a widely-used MPR heuristic, and we show that our trained policies are able to efficiently cover the network while bypassing the MPR set selection process. Our approach promises a first step toward bolstering the resilience of real-world broadcast communication infrastructures via learned, collaborative information dissemination.

Introduction

Nowadays, group communication, implemented in a broadcast or multicast fashion, finds a natural application in different networking scenarios, such as Vehicular Ad-hoc Networks (VANETs) (Tonguz et al. 2007; Ibrahim, Toycan, and Mawlood 2020), with the necessity to disseminate information about the nodes participating, e.g. identity, status, and position, or crucial events happening in the network. These systems can be characterized by congestion-prone networks and/or different resource constraints, such that message dissemination becomes considerably expensive if not adequately managed. For this matter, message forwarding calls for scalable and distributed solutions able to minimize the total number of forwards, while achieving the expected coverage. Moreover, modern broadcast communication protocols often require careful adjustments of their parameters before achieving adequate forwarding policies, which would otherwise result in sub-optimal performance in terms of delivery ratio and latency (Suri et al. 2022).

Recently, researchers have considered learning communication protocols (Foerster et al. 2016) with Multi-Agent Reinforcement Learning (MARL) (Buşoniu, Babuška, and De Schutter 2010). At its core, MARL seeks to design systems where multiple agents learn to optimize their objective by interacting with the environment and the other entities involved. Such tasks can be competitive, cooperative, or a combination of both, depending on the scenario. As agents interact within a shared environment, they often find the need to exchange information to optimize their collective performance. This has led to the development of communication protocols that are learned rather than pre-defined, allowing agents to evolve their own "language" or signaling system.

Nevertheless, learning to communicate with MARL comes with several challenges. In multi-agent systems, actions taken by one agent can significantly impact the rewards and state transitions of other agents, rendering the environment more complex and dynamic, and ensuring that agents develop a shared and consistent communication protocol, is an area of active research. Methods such as CommNet (Sukhbaatar, Szlam, and Fergus 2016) and BiCNet (Peng et al. 2017), focus on the communication of local encodings of agents' observations. These approaches allow agents to share a distilled version of their individual perspectives, enabling more informed collective decision-making. ATOC (Jiang and Lu 2018) and TarMAC (Das et al. 2019) have ventured into the realm of attention mechanisms. By leveraging attention, these methods dynamically determine which agents to communicate with and what information to share, leading to more efficient and context-aware exchanges. Yet another approach, as exemplified by DGN (Jiang et al. 2020), harnesses the power of Graph Neural Networks (GNNs) to model the interactions and communications between agents. By representing the multi-agent system as a graph, DGN captures the complex relations between agents, facilitating the emergence of effective strategies even when constrained communication may limit the range of cooperation.

However, to the best of our knowledge, no MARL-based method involving active communication by the agents and Graph Convolution has been proposed to address the unique challenges of optimizing the process of information dissemination within a broadcast network.

Contributions In this work, we propose an **innovative cooperative MARL formulation for information dissemination** where agents learn in a Centralized Training Decentralized Execution (CTDE) (Gronauer and Diepold 2022) fashion. Each agent independently decides whether (and when) to forward a message or not, based on their one-hop neighbor structure, the number of neighbors each neighbor has, and the behavior of their neighborhood.

Furthermore, we design, implement, and test **two different architectures, namely Local-DGN, and Hyperlocal-DGN**, which require different levels of communication between the agents and leverage the power of Graph Convolutional Reinforcement Learning and Graph Attention Network (GAT) with dynamic attention to capture essential network features and relations between the agents.

We carry out an **experimental study** which shows the effectiveness of MARL-based solutions on a series of static graphs, achieving **network coverage with reduced communication overhead** when empirically compared to a well-established Multi Point Relay (MPR) heuristic employed in broadcast protocols and a MARL baseline.

The impact of our data-driven approach is particularly heightened by the existence of network simulators capable of replicating real-world scenarios, such as NS-3 (Riley and Henderson 2010), which in turn facilitate the training of the agents. By shedding light on the potential of learning-based approaches in addressing information dissemination challenges, our work underscores the versatility of MARL in present and future, real-world applications such as information dissemination in social networks (Guille et al. 2013), space networks (Ye and Zhou 2021), and vehicle-safety-related communication services (Ma et al. 2012).

Background

Reinforcement Learning In Reinforcement Learning (RL) (Sutton and Barto 2018) agents observe the state of the environment and interact with it, receiving reward signals to improve their decision-making process. In this way RL, provides solutions for sequential decision-making problems formulated as Markov Decision Processs (MDPs) (Puterman 1994). The Partially Observable Markov Decision Process (POMDP) represents a natural extension of the MDP framework to scenarios where agents have limited or partial observability of the underlying environment. Formally, a POMDP can be represented as $\langle \mathcal{S}, \mathcal{A}, \mathcal{O}, p, \mathcal{R}, \mathcal{Z}, \gamma \rangle$, where \mathcal{S} and \mathcal{A} denote the state and action spaces, respectively, and \mathcal{O} is the set of observations, that is, the imperfect or noisy information received by the agents regarding the current state. The agent’s action at time t , $a_t \in \mathcal{A}(s_t)$, taken in state $s_t \in \mathcal{S}$ results in a reward signal $r_{t+1} \in \mathcal{R} \subset \mathbb{R}$ and a transition to a new state s_{t+1} with a probability distribution $p(s_{t+1}, r_{t+1} | s_t, a_t) : \mathcal{S} \times \mathcal{R} \times \mathcal{S} \times \mathcal{A} \rightarrow [0, 1]$. \mathcal{Z} represents the observation function that maps the true state to the observed state for each agent. Finally, γ is a discount factor modeling how much the agent cares about future rewards w.r.t. present ones. Due to the uncertainty introduced by partial observability, agents need to maintain belief states, which are probability distributions over the true states, and

make decisions based on these belief states. To this end, several methods have been proposed such as Deep Recurrent Q-Learning (Hausknecht and Stone 2015).

Multi-Agent Reinforcement Learning For multi-agent systems, the RL paradigm extends to MARL (Buşoniu, Babuška, and De Schutter 2010), where multiple entities, potentially learners or non-learners, interact with the environment. In this context, the generalization of POMDPs leads to Decentralized Partially Observable Markov Decision Process (Dec-POMDP), characterized by the tuple $\langle \mathcal{I}, \mathcal{S}, \mathcal{A}_{i \in \mathcal{I}}, \mathcal{P}, \mathcal{R}_{i \in \mathcal{I}}, \mathcal{O}_{i \in \mathcal{I}}, \gamma \rangle$. Here, \mathcal{I} represents the set of agents, \mathcal{S} denotes the state space with an initial state s_0 , $\mathcal{A}_{i \in \mathcal{I}}$ stands for the action space for each agent, \mathcal{P} is the joint probability distribution over the next state given the current state and joint action, $\mathcal{R}_{i \in \mathcal{I}}$ denotes the reward function for each agent, and $\mathcal{O}_{i \in \mathcal{I}}$ represents the set of observations for each agent. Several MARL algorithms have been presented in the literature, addressing different tasks (cooperative, competitive, or mixed) and pursuing different learning goals such as stability or adaptation (Buşoniu, Babuška, and De Schutter 2010; Gronauer and Diepold 2022; Ahmed et al. 2022).

Graph Neural Networks GNNs (Scarselli et al. 2009) directly process graph structures, handling neighborhoods of variable size, and enabling different prediction levels, e.g. at the graph, node, or edge level. This is achieved by combining function approximators such as Neural Networks (NNs) with a *Message Passing* mechanism, where a node x_i aggregates over the immediate neighbors features and combines its own features with the aggregated information. Repeating this operation N times, it convolves information over nodes N hops away. GNNs have shown remarkable success in several domains, such as recommendation systems, drug discovery, computer vision, natural language processing, and social network analysis. Recent advancements in GNN research have introduced novel architectures, such as Graph Convolutional Network (GCN) (Kipf and Welling 2017), GraphSAGE (Hamilton, Ying, and Leskovec 2017), and GAT (Veličković et al. 2018), which have improved the performance of GNNs in various tasks. In this paper, we use GATs with dynamic attention (Brody, Alon, and Yahav 2022) to capture relevant features of communication networks.

Graph Convolutional Reinforcement Learning In Graph Convolutional Reinforcement Learning (Jiang et al. 2020), the dynamics of multi-agent environments are represented as a graph, where each agent is a node with a set of neighbors determined by specific metrics. In this approach, a key role is played by Relation Kernels and their capability to merge features within an agent’s receptive field, all while capturing detailed interactions and relationships between agents. Building upon this foundation, the DGN architecture is defined as integrating an observation encoder, convolutional layers, and a Q-network. During training, a batch of experiences \mathcal{B} is sampled and the following loss is minimized:

$$L(\theta) = \frac{1}{|\mathcal{B}|} \sum_{\mathcal{B}} \frac{1}{N} \sum_{i=1}^N (y_i - Q(O_{i,C}, a_i; \theta))^2 \quad (1)$$

where N is the number of agents, and $O_{i,C}$ is the observation of agent i with the respective adjacency matrix C . Furthermore, to maintain the consistency of relations learned over several timesteps, a Temporal Relation Regularization term is added to the loss. Empirical evaluations showcased DGN’s effectiveness in fostering cooperative and sophisticated strategies in numerous traditional benchmarks. In this paper we build on the DGN framework and design novel MARL architectures for optimizing information dissemination in broadcast networks.

Related Work

The Optimized Link State Routing (OLSR) (Clausen and Jacquet 2003; Dearlove and Clausen 2014) protocol is a proactive routing protocol used in Mobile Ad-hoc Networks (MANETs) and, more in general, wireless mesh networks. While being a comprehensive routing protocol implementing different functionalities, OLSR uses a technique called **MPR selection** (Qayyum, Viennot, and Laouiti 2002; Adjih, Jacquet, and Viennot 2005) to optimize information dissemination throughout a broadcast network.

Thanks to the exchange of "HELLO messages" present in OLSR, nodes are able to discover information about their two-hop neighborhood and designate specific one-hop neighbors as responsible to forward information they transmit, namely their MPR set. A greedy selection algorithm is employed by default in the standard OLSR implementation (Clausen and Jacquet 2003) to define the MPR sets. This algorithm selects neighbors that can encompass the largest segments of node i 's two-hop neighborhood, ensuring an exhaustive reach to all two-hop neighbors while circumventing indiscriminate network flooding. Further details regarding the overhead caused by this process are presented in the Experiments Section.

In this paper, we tackle optimized information dissemination on broadcast networks and use the traditional selection algorithm employed by OLSR as a baseline¹. However, we define a completely different approach that leverages MARL to produce a policy that, once trained, can be used in each node to determine whether to forward a message or not.

Very recent work has considered MARL approaches in the context of communication networks (Yahja et al. 2022; Kaviani et al. 2021, 2023). The more closely related to the presented work is DeepMPR presented in (Kaviani et al. 2023) which addresses the optimization of goodput (bits of useful data delivered at target location per unit of time) in dynamic multicast networks. While related, both the problem considered and the approach taken here are different. We consider static broadcast networks and focus on coverage and the size of the associated Connected Dominating Set (CDS) rather than goodput. Moreover, in contrast to (Kaviani et al. 2023) where the proposed method utilizes PPO (Schulman et al. 2017), we design two novel approaches based on the integration of GATs for capturing essential local features and relations among agents.

¹The complete MPR selection algorithm used by OLSR is shown in Algorithm 1 in the Supplementary Materials.

Optimized Flooding in Broadcast Networks

Let us consider a broadcast network where each device is a radio. Each radio can be viewed as a node with a radius of influence, representing a certain distance or proximity within which transmitted information is received. Given a broadcast network and a radius of influence r , we can, thus, define the associated graph $\mathcal{G} = (\mathcal{V}, \mathcal{E})$, where the node set \mathcal{V} corresponds to the set of radios in the network and the set of edges $\mathcal{E} = \{(u, v) | u, v \in \mathcal{V}, \text{distance}(u, v) \leq r\}$, where $\text{distance}(u, v)$ is a distance metric that measures the spatial or logical distance between nodes u and v . For every node $v \in \mathcal{V}$, the set of its neighbors is defined as $\mathcal{N}_v = \{u \in \mathcal{V} | (v, u) \in \mathcal{E}\}$.

A main objective of broadcast communications over connected networks is called optimized flooding (Qayyum, Viennot, and Laouiti 2002) and, is achieved when the information emitted from a given node $v \in \mathcal{V}$ reaches every other node $u \neq v$, thanks to forwarding actions of a set of nodes $\mathcal{D} \subseteq \mathcal{V}$. While maximizing coverage it is also desirable to minimize redundant transmissions, which might impact resource utilization, such as bandwidth, power consumption, and latency. Form a graph-theoretic point, of view this can be achieved by identifying a specific subset of nodes, called a dominating set, that will be tasked with retransmitting the information.

More formally, given a graph $\mathcal{G} = (\mathcal{V}, \mathcal{E})$, a *dominating set* $\mathcal{D} \subseteq \mathcal{V}$ is a subset of nodes such that, for every node $v \in \mathcal{V}$, either v is in \mathcal{D} or v has at least one neighboring node in \mathcal{D} . To ensure that the broadcast packet reaches all nodes in the network, it is essential for the dominating set to be connected, that is to have a path between any two nodes comprising only nodes in the set. Finally, transmission redundancy is minimized for Minimum Connected Dominating Sets (MCDSs), that is, Connected Dominating Sets of minimum size.

Two main challenges arise from a flooding approach purely based on computing a MCDS: first, this task is a known NP-complete problem, as vertex cover can be reduced to the problem of computing a connected dominating set (Garey and Johnson 1979); furthermore, it requires the introduction of a centralized entity which is highly undesirable.

A much more efficient and realistic approach is to approximate the minimum connected dominating set in a distributed manner, relying only on local observations of the network made from each node's perspective. Indeed, this is the approach taken by the MPR selection (Adjih, Jacquet, and Viennot 2005) heuristic, as well as the MARL-based approach we present here.

MARL-based Optimized Flooding

In this section, we describe a novel approach for optimizing information flooding in broadcast networks that is based on a MARL formulation and a learning approach inspired by Graph Convolutional Reinforcement Learning. We start by presenting our formulation of the optimized flooding problem as a Dec-POMDP and then introduce Local and Hyperlocal Relational Kernels, which are at the core of our two algorithms, respectively, Local-DGN and Hyperlocal-DGN. We design our methods to achieve efficient dissemination while requiring different degrees of communication.

MARL Formulation

A decentralized approach to network flooding optimization can be naturally mapped into a Dec-POMDP. Nodes correspond to agents, while the available actions are to either forward a message or not. A reasonable assumption is that the agents are able to discover their one-hop neighbors and gather information about their two-hop neighbors, thanks to an underlying communication protocol, such as OLSR (Clausen and Jacquet 2003; Dearlove and Clausen 2014). In our formulation, agents are allowed to know only the number of neighbors each of its neighbors is connected to, differently from OLSR and its MPR heuristic that needs to obtain a complete two-hop knowledge of the network. A reward signal is issued to each agent and it is defined in terms of its 2-hop coverage. Penalties are also applied to the reward, based on the number of messages sent by the agent’s neighborhood or the coverage potential of the neighborhood, respectively whether the agent has forwarded or not.

Moreover, it is clear that a node is able to participate in the process, i.e. become “active”, only once it receives the message and that it can be a meaningful actor only for a limited number of steps of the overall dissemination process, that is, for the portion of it that impacts its neighborhood. We capture this by limiting the agent’s active state to a fixed, few number of steps which we call *local horizon*.

In line with the Dec-POMDP literature, we envision the dissemination process discretized into (time) steps and starting with a source node transmitting a data message to its immediate neighbors. We also assume that active agents are able to synchronize their behavior so that their next step will be taken simultaneously.

More specifically, given the broadcast network represented by graph $\mathcal{G} = (\mathcal{V}, \mathcal{E})$ and node $s_0 \in \mathcal{V}$, we define the Dec-POMDP associated to the optimized flooding of \mathcal{G} with source s_0 , as $\langle \mathcal{I}, \mathcal{S}, \mathcal{A}_{i \in I}^i, \mathcal{P}, \mathcal{R}_{i \in I}^i, \mathcal{O}_{i \in I}^i, \gamma \rangle$, where:

Agents set \mathcal{I} . Set \mathcal{I} contains one agent for each node in \mathcal{V} . During training, \mathcal{I} is divided into three disjoint sets which are updated at every timestep t : the active set $\mathcal{I}_a(t)$, the done set $\mathcal{I}_d(t)$, and the idle set $\mathcal{I}_i(t)$. Agents in $\mathcal{I}_i(t)$ are inactive because they have not received the message yet. At the beginning of the process, $\mathcal{I}_i(t)$ will contain all agents except the one associated with s_0 . Agents in $\mathcal{I}_d(t)$ are also inactive, but they already took part in the current game and terminated their experience. $\mathcal{I}_a(t)$, instead, includes the set of agents actively participating in the game at t . Agents in $\mathcal{I}_i(t)$ are moved to \mathcal{I}_a at time step $t+1$, if they have received a message. We assume agents have an internal counter which is initialized with the local horizon value and activated when they transition from $\mathcal{I}_i(t)$ to $\mathcal{I}_a(t)$. The agents decrease their counter by one after each subsequent time step until the counter reaches value 0, at which point they are moved to \mathcal{I}_d .

Actions $\mathcal{A}_{i \in I}^i$ and transition probability \mathcal{P} . For any time step t , if agent i is in $\mathcal{I}_a(t)$, then, \mathcal{A}^i contains two possible actions: forward the information to their neighbors or stay idle. Active agents are allowed to forward the information multiple times. Agents in $\mathcal{I}_i(t)$ and $\mathcal{I}_d(t)$ do not participate in the decision-making process, hence their action set is empty, for

Node	# Neighbours	Data Messages	A_1	A_2	A_3	A_4
2	3	0	0	0	0	0
4	1	1	1	0	0	0
5	3	1	0	0	1	0
7	4	0	0	0	0	0

Table 1: Example of features in the one-hop observation of node 5 seen in Figure 1.

any t . If an agent forwards a message, each of its neighbors will receive it. This means that function \mathcal{P} is deterministic and maps the current state into a state where all the neighbors of active nodes that have chosen to forward, which had not received the message, if any, are now covered.

Observations $\mathcal{O}_{i \in I}^i$ and State \mathcal{S} . Each node in the graph has a set of six features, including its number of neighbors, the number of messages transmitted, and its action history. The latter identifies in which, if any, of its active turns, the agent forwarded the message. Assuming the local horizon is equal to k , this last feature can be represented as a binary array of size k . An agent’s observations include its features and those of its one-hop neighbors. Table 1 shows, as an example, the features included in the observation of Node 5 in the network shown in Figure 1 (left). In our setting, a state corresponds to the network’s graph \mathcal{G} , the features of each node and a partition of \mathcal{V} in those who have received a message and those who have not. We notice that the latter information is only partially visible to agents, even within their neighborhood. In fact, an agent cannot tell if a neighbor that has not forwarded yet has received the message or not.

Rewards $\mathcal{R}_{i \in I}^i$. At the end of each step every agent is issued with a reward signal. Such signals are made of two main components, a positive and a negative reward. The positive term rewards the agent based on its two-hop coverage, i.e. how many one- and two-hop neighbors have been covered, capturing the ability of observable (the agent’s neighborhood) and unobservable agents to contribute to the dissemination task. One of two different penalties might be issued, based on the agent’s behavior. If the agent has ever forwarded the message, it will participate in a “neighborhood shared transmission cost” punishing the agent for the number of forwards sensed in its neighborhood. Otherwise, it will receive penalties based on the “coverage potential” of neighbors that have not yet received the information. The reward signal for agent i at time t can, thus, be depicted as follows:

$$r_{i,t} = \frac{v(\mathcal{N}(\mathcal{N}_i), t)}{|\mathcal{N}(\mathcal{N}_i)|} - p(i, t) \quad (2)$$

$$p(i, t) = \begin{cases} m(\mathcal{N}_i, t), & \text{if } i \in \mathcal{T}(t) \\ \mu(\mathcal{N}_i, t), & \text{if } i \in \mathcal{S}(t) \end{cases} \quad (3)$$

In Equation 2, $\mathcal{N}(\mathcal{N}_i)$ represents the set of two-hop neighbors of agent i , $v(\mathcal{N}(\mathcal{N}_i), t)$ represents the number of them that by timestep t have already received the message, while $p(i, t)$, defines the penalties assigned to that agent. The latter

is further described in Equation 3, where $\mathcal{T}(t)$ is the set of active agents that have forwarded the message at least once, while $\mathcal{S}(t)$ is the set of active agents that have not forwarded the message yet. $m(\mathcal{N}_i, t)$ denotes the number of messages transmitted by the neighborhood of agent i at timestep t . $\mu(\mathcal{N}_i, t)$ instead defines the coverage potential of node i , which we define as $\max(\{|\mathcal{N}_j| : j \in \mathcal{N}_i, j \notin \mathcal{R}(t)\})$, where $\mathcal{R}(t)$ is the set of agents that have received the message.

We note that by assessing the ability of an agent's neighborhood to reach nodes beyond its immediate neighbors, the positive term depicted in Equation 2, encourages agents to collectively cover more nodes through coordination within their vicinity. On the other hand, the neighborhood shared transmission cost reinforces the distributed collaboration among agents by steering agents away from redundancy and promoting efficient collaboration. Finally, the coverage potential counterbalances the shared transmission costs, by hastening transmission to nodes with highly populated neighborhoods that have not yet been reached.

Local Relation Kernels

Our approach is based on Relation Kernels, a fundamental component of Graph Convolutional Reinforcement Learning (Jiang et al. 2020), which the same authors implemented in their proposed DGN model.

In DGN, Graph Convolutional Layers play a crucial role in integrating feature vectors associated to nodes within a local region around a node i , by generating a latent feature vector h_i^t comprising node i and its neighboring nodes. By adding more convolutional layers, the receptive field of an agent expands progressively, leading to the accumulation of more information. Consequently, the scope of cooperation also broadens, enabling agents to collaborate more effectively. Specifically, with one convolutional layer, node i aggregates the features of the nodes in its one-hop neighborhood \mathcal{N}_i . When two layers are stacked, node i receives the output of the first convolutional layer of nodes in its one-hop neighborhood, which, in turn, embeds information from nodes two hops away from i . Notably, irrespective of the number of convolutional layers, node i only communicates with its one-hop neighbors, making DGN practical in real-world scenarios.

We adapt this approach to broadcast networks where agents can exploit the underlying communication protocol to share their neighborhood embedding, instead of the MPR set, with their one-hop neighbors. This is beneficial in different ways: first, as we already mentioned, the dissemination of such embeddings enables cooperation; furthermore, it hinders agents from sharing explicit information about their neighborhood while exploiting the expressiveness of the embeddings.

Local Horizon and n-step TD Estimation During training, at each timestep, the tuple $(\mathcal{O}_{\mathcal{I}_a}, \mathcal{A}_{\mathcal{I}_a}, \mathcal{R}_{\mathcal{I}_a}, \mathcal{O}'_{\mathcal{I}_a})$ is stored in a circular replay buffer with fixed length. $\mathcal{O}_{\mathcal{I}_a}$ indicates the set of observations of all agents in \mathcal{I}_a at the current timestep, $\mathcal{A}_{\mathcal{I}_a}$ the set of actions taken by the agents in \mathcal{I}_a at the current timestep, $\mathcal{R}_{\mathcal{I}_a}$ is the set of rewards associated to the experience, and $\mathcal{O}'_{\mathcal{I}_a}$ the set of observations of agents in \mathcal{I}_a at the next timestep.

At each training step, we sample a random batch \mathcal{B} from

the replay buffer, with every sample $(o_t, a_t, r_t, o_{t+1}) \in \mathcal{B}$ representing the experience of a single agent. We then minimize the loss computed in a Double Deep Q Networks (DDQNs) (Hasselt, Guez, and Silver 2016) fashion:

$$\mathcal{L}(\theta) = \frac{1}{|\mathcal{B}|} \sum_{(o_t, a_t, r_t, o_{t+1}) \in \mathcal{B}} \left[(y_t - Q(o_t, a_t; \theta))^2 \right], \quad (4)$$

where y_t is the target return and $Q(o_t, a_t; \theta)$ the predicted Q value, parameterized with θ , given the current observation and action. We note that this loss is different from the one employed in DGN which instead is not focused on a single agent but considers all of the agents.

Training is performed at a regular frequency every m steps. Additionally, we perform n -step Temporal Difference (TD) estimation, with n equal to the local horizon (k).

We note that if the replay buffer contains the remaining steps until the local horizon is reached, the n -step computation serves an unbiased value of the return, such that:

$$y_t = \sum_{i=0}^{k-t} \gamma^i r_{t+i}. \quad (5)$$

Otherwise, if the trajectory stored in the buffer contains only the next j steps before termination, y_t will be estimated as:

$$y_t = \sum_{i=0}^{j-1} \gamma^i r_{t+i} + \gamma^j Q(s_{t+i}, \text{argmax}_{a'} Q(s_{t+i}, a'; \theta); \bar{\theta}), \quad (6)$$

where θ is the current network and $\bar{\theta}$ is the target network.

Policy Parameterization Our novel Local-DGN architecture, depicted in Figure 1, consists of an encoder module comprised of three different stages: one Multi Layer Perceptron (MLP) followed by two multi-headed GATs (Veličković et al. 2018) with dynamic attention (Brody, Alon, and Yahav 2022). The final latent representation will comprise the concatenation of each stage output, which is then fed to a dueling network (Wang et al. 2016) decoding the final representation into the predicted Q values.

For each agent i in the network, following the MLP encoding stage such that the features of agent i are projected into a learned representation \mathbf{x}_i , the output of each of the first GAT's attention heads, $m \in M$, will be:

$$\mathbf{x}_i^m = \alpha_{i,i}^m \mathbf{W} \mathbf{x}_i + \sum_{j \in \mathcal{N}(i)} \alpha_{i,j}^m \mathbf{W} \mathbf{x}_j \quad \forall m \in M \quad (7)$$

where the dynamic attention α^m for the tuple (i, j) , denoted as $\alpha_{i,j}^m$, is computed by:

$$\alpha_{i,j}^m = \frac{\exp(\mathbf{a}^\top \text{LeakyReLU}(\mathbf{W}[\mathbf{x}_i \| \mathbf{x}_j]))}{\sum_{k \in \mathcal{N}_i \cup \{i\}} \exp(\mathbf{a}^\top \text{LeakyReLU}(\mathbf{W}[\mathbf{x}_i \| \mathbf{x}_k]))}. \quad (8)$$

where \mathbf{a} and \mathbf{W} are learned. We denote $\hat{\mathbf{X}}_i = \mathbf{x}_i^0 \| \mathbf{x}_i^1 \| \dots \| \mathbf{x}_i^m$, where $\|$ is the concatenation operator, as

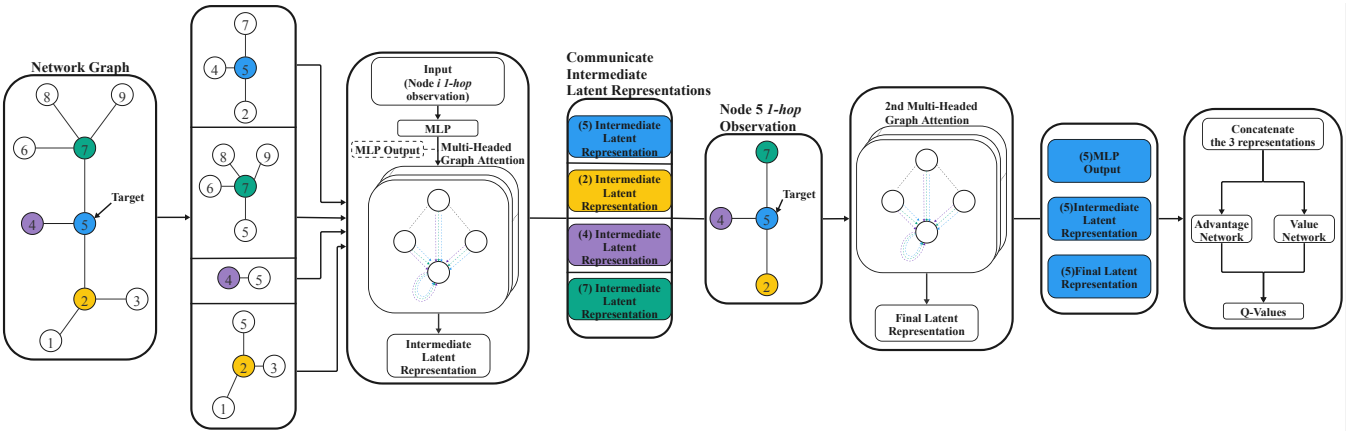


Figure 1: The Local-DGN (L-DGN) architecture.

the concatenation of every attention output and observe that, at this point, each agent i is in possession of an intermediate latent representation $\hat{\mathbf{X}}_i$. These representations are fed to the second and last GAT layer with dynamic attention, producing the output $\hat{\mathbf{Z}}_i$.

Finally, the output of each encoding stage is concatenated in a final latent representation \mathbf{H}_i :

$$\mathbf{H}_i = \mathbf{x}_i \parallel \hat{\mathbf{X}}_i \parallel \hat{\mathbf{Z}}_i. \quad (9)$$

The L-DGN architecture harmoniously integrates with the communication process present in protocols such as OLSR. Every agent feeds its own features and the ones describing its one-hop neighbors, first to the MLP stage, and then to the first GAT stage. Following such a process, every agent then shares their intermediate representation $\hat{\mathbf{X}}_i$ with their one-hop neighbors. Once such representations are collected, the agents feed such intermediate representations to the second GAT layer, extracting the final output \mathbf{H}_i .

In the last stage, \mathbf{H}_i is fed to the two separate streams of the dueling network, namely the advantage network A and the value network V , implemented by two separate MLPs. The predicted Q values are then obtained by integrating the output of the two dueling networks:

$$Q(o_t, a_t) = V(\mathbf{H}_i) + \left(A(\mathbf{H}_i) - \frac{1}{|A(\mathbf{H}_i)|} \sum_{a'} A(\mathbf{H}_i) \right). \quad (10)$$

Although our Local-DGN approach enables efficient cooperation with the exchange of latent representations, the process of exchanging such embeddings still generates communication overhead. This observation leads us to consider the following hypothesis: Can we limit the exchange of information within a neighborhood to the single integer representing the number of each agent's neighbors, while still achieving cooperation?

Hyperlocal Relation Kernels

With the objective of avoiding extra communication, we design a second model, named Hyperlocal-DGN (HL-DGN),

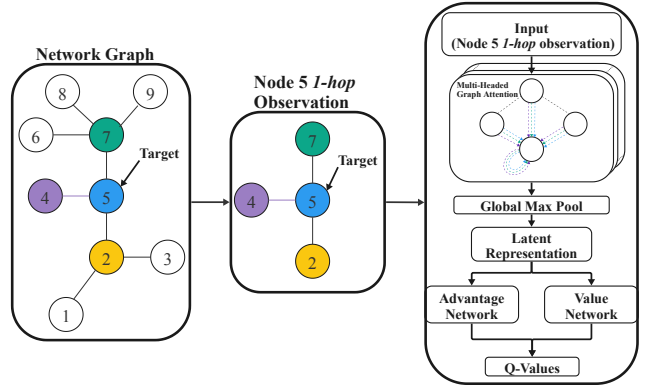


Figure 2: The Hyperlocal-DGN (HL-DGN) architecture.

which, as shown in Figure 2, resembles L-DGN in its form. We replace the three encoding stages with a single GAT layer with dynamic attention, followed by a global max-pooling layer. Inspired by the application of max-pooling layers in Convolutional Neural Networks (CNNs) (Cireşan et al. 2011), we aim at providing the dueling network with a new latent representation that can be interpreted as a global representation of the agent's i observation, encapsulating the salient attention-weighted features of its neighbors. The intuition behind using global pooling layers is that agents could still produce rational decisions based only on the features of the observed neighborhood and the neighboring agents' behavior, and avoiding the communication of their latent representations, as seen, instead, in Local Relation Kernels.

Given an observation o_i , comprising the one-hop local graph of agent i , we feed this graph to the GAT layer and produce a set of latent representation $\hat{\mathbf{Y}}_j, \forall j \in \mathcal{N}_i \cup \{i\}$. Then we perform the global max pooling operation, such that:

$$\mathbf{H}_i = \text{ReLU}(\max_{j \in \mathcal{N}_i \cup \{i\}} \hat{\mathbf{Y}}_j). \quad (11)$$

Finally, \mathbf{H}_i is fed to the dueling network following the same process depicted in Equation 10.

Nodes	Method	Coverage	Data Messages	Control Overhead
20	MPR	100%	12.05	60
	DGN-R	100%	21.06	60
	L-DGN	99.95%	11.84	60
	HL-DGN	100%	13.17	40
50	MPR	100%	30.8	150
	DGN-R	99.98%	60.65	150
	L-DGN	93.3%	25.42	150
	HL-DGN	100%	35.1	100

Table 2: Method comparison in terms of Coverage, Data Messages, and Control Overhead for both testing topologies sets.

Experiments

A first set of 50K connected static graph topologies is generated, with 20 nodes per graph, and no constraints on the number of one-hop neighbors. In addition, two separate sets of 100 topologies are used for testing, respectively with 20 and 50 nodes per graph. When training, the environment selects a random graph, as well as a random node to be the source of the information to disseminate. During testing a precise node is systematically chosen to be the source in order to encourage reproducibility and coherence of the results. In our experiments, we set the value of the local horizon to 4.

We conduct a comprehensive comparative analysis involving our two novel methodologies, namely L-DGN and HL-DGN, alongside the MPR heuristic, and DGN-R, the variant of DGN (Jiang et al. 2020) that does not include Temporal Relation Regularization, which is not required in our setting where agent interaction is temporally bounded by a short local-horizon. To ensure an equitable evaluation, we maintain consistent hyperparameters and layer dimensions for each layer type across all three models. The reader can refer to the Training Performance, Hyperparameters, and Ablation Study sections of the Supplementary Materials for further details.

In both our proposed methodologies and the DGN-R model, we employ GAT with dynamic attention. In the original DGN implementation, the authors employ a transform-like dot product as part of their relation kernel. Although it has been demonstrated that this method does indeed compute dynamic attention, it is inherently less powerful than GAT with dynamic attention in capturing such intricacies (Brody, Alon, and Yahav 2022).

Our framework, including the graph topologies used for training and testing, is accessible on GitHub². The reader can refer to the Implementation Details and Hardware Involved section of the Supplementary Material for further details regarding the hardware involved, the libraries employed, and how to reproduce our results.

Control Overhead We note that, in our setting, all the nodes begin the process simultaneously and, due to assumed perfect synchronization among nodes, every node diffuses

information at precisely the same time. To this end, a "bootstrap phase" is defined, during which nodes engage in two successive rounds of "HELLO" messages, each serving a distinct purpose. The first round establishes the presence of nodes and forms initial network connectivity. In the second round, nodes exchange the acquired information within their one-hop neighborhood, leading to each node gaining knowledge of their two-hop neighborhood. We note that the information exchanged between the nodes in this phase depends on the approach being used (i.e., neighbors' ids for MPR, and neighborhood size for all other methods). After this bootstrap phase, a third round is dedicated to broadcasting pre-calculated MPR sets or latent representations for, respectively, MPR selection and L-DGN or DGN-R. Summarizing, the MPR heuristic, DGN-R, and L-DGN, all demonstrate a control message overhead proportional to three times the number of nodes, while HL-DGN demonstrates an overhead scaled down to two times the node count, thanks to the absence of the third round of HELLO messages.

Results In Table 2 we show our results in terms of average network coverage, average number of data messages (that is, containing the actual information to be disseminated), and control overhead. For the graphs with 20 nodes, the MPR heuristic attains full coverage (100%) while employing a data message count of 12.05. The DGN-R model achieves complete coverage with the highest average message count of 21.06. In contrast, the proposed L-DGN model maintains a high coverage rate of 99.95%, utilizing a comparatively lower message count of 11.84. Additionally, the HL-DGN model successfully attains an impressive full coverage while employing 13.17 messages and one less round of HELLO messages. Turning attention to the graph with 50 nodes, the MPR heuristic once again accomplishes full coverage (100%), with a data message count of 30.8. The DGN-R model, while achieving a slightly reduced coverage rate of 99.98%, employs 60.65 data messages. The L-DGN model demonstrates a decrease in coverage rate, reduced to 93.3% with 25.42 data messages. The HL-DGN model again sustains full coverage with a message count of 35.1. We conjecture that this may be thanks to a reduced inhibitory effect of the neighborhood-shared transmission cost on HL-DGN, where neighbors are unable to deflect the agent by sharing that their neighborhood cost is already too high.

In summary, the results underscore the efficacy of the proposed L-DGN and HL-DGN models in outperforming the MARL baseline and in achieving competitive coverage while optimizing message utilization against a widely used MPR heuristic.

Future Work

Our future work will extend beyond the current framework, delve into more complex settings such as dynamic graphs, and agent observations enhanced with additional information provided by protocols such as OLSR. Orthogonally, we will investigate the application of our approach beyond broadcast networks to the dissemination of information in domains with higher levels of abstraction, such as social networks.

²Repository available at <https://github.com/RaffaeleGalliera/melissa>

References

Adjih, C.; Jacquet, P.; and Viennot, L. 2005. Computing connected dominated sets with multipoint relays. *Ad Hoc & Sensor Wireless Networks*, 1(1-2): 27–39.

Ahmed, I. H.; Brewitt, C.; Carlucho, I.; Christianos, F.; Dunion, M.; Fosong, E.; Garcin, S.; Guo, S.; Gyevnar, B.; McInroe, T.; Papoudakis, G.; Rahman, A.; Schäfer, L.; Tamborski, M.; Vecchio, G.; Wang, C.; and Albrecht, S. V. 2022. Deep reinforcement learning for multi-agent interaction. *AI Commun.*, 35(4): 357–368.

Brody, S.; Alon, U.; and Yahav, E. 2022. How Attentive are Graph Attention Networks? In *International Conference on Learning Representations (Poster)*.

Bušoniu, L.; Babuška, R.; and De Schutter, B. 2010. *Multi-agent Reinforcement Learning: An Overview*, 183–221. Berlin, Heidelberg: Springer Berlin Heidelberg. ISBN 978-3-642-14435-6.

Cireşan, D. C.; Meier, U.; Masci, J.; Gambardella, L. M.; and Schmidhuber, J. 2011. Flexible, High Performance Convolutional Neural Networks for Image Classification. In *Proceedings of the Twenty-Second International Joint Conference on Artificial Intelligence - Volume Volume Two*, IJCAI’11, 1237–1242. AAAI Press. ISBN 9781577355144.

Clausen, T. H.; and Jacquet, P. 2003. Optimized Link State Routing Protocol (OLSR). RFC 3626.

Das, A.; Gervet, T.; Romoff, J.; Batra, D.; Parikh, D.; Rabbat, M.; and Pineau, J. 2019. TarMAC: Targeted Multi-Agent Communication. In Chaudhuri, K.; and Salakhutdinov, R., eds., *Proceedings of the 36th International Conference on Machine Learning*, volume 97 of *Proceedings of Machine Learning Research*, 1538–1546. PMLR.

Dearlove, C.; and Clausen, T. H. 2014. Optimized Link State Routing Protocol Version 2 (OLSRv2) and MANET Neighborhood Discovery Protocol (NHDP) Extension TLVs. RFC 7188.

Fey, M.; and Lenssen, J. E. 2019. Fast Graph Representation Learning with PyTorch Geometric. In *ICLR Workshop on Representation Learning on Graphs and Manifolds*.

Foerster, J. N.; Assael, Y. M.; de Freitas, N.; and Whiteson, S. 2016. Learning to Communicate with Deep Multi-Agent Reinforcement Learning. In *Proceedings of the 30th International Conference on Neural Information Processing Systems*, NIPS’16, 2145–2153. Red Hook, NY, USA: Curran Associates Inc. ISBN 9781510838819.

Garey, M. R.; and Johnson, D. S. 1979. *Computers and Intractability: A Guide to the Theory of NP-Completeness*. W. H. Freeman. ISBN 0-7167-1044-7.

Gronauer, S.; and Diepold, K. 2022. Multi-agent deep reinforcement learning: a survey. *Artif. Intell. Rev.*, 55(2): 895–943.

Guille, A.; Hacid, H.; Favre, C.; and Zighed, D. A. 2013. Information Diffusion in Online Social Networks: A Survey. *SIGMOD Rec.*, 42(2): 17–28.

Hamilton, W. L.; Ying, R.; and Leskovec, J. 2017. Inductive Representation Learning on Large Graphs. In *Proceedings of the 31st International Conference on Neural Information Processing Systems*, NIPS’17, 1025–1035. Red Hook, NY, USA: Curran Associates Inc. ISBN 9781510860964.

Hasselt, H. v.; Guez, A.; and Silver, D. 2016. Deep Reinforcement Learning with Double Q-Learning. In *Proceedings of the Thirtieth AAAI Conference on Artificial Intelligence*, AAAI’16, 2094–2100. AAAI Press.

Hausknecht, M. J.; and Stone, P. 2015. Deep Recurrent Q-Learning for Partially Observable MDPs. In *2015 AAAI Fall Symposia, Arlington, Virginia, USA, November 12-14, 2015*, 29–37. AAAI Press.

Ibrahim, B. F.; Toycan, M.; and Mawlood, H. A. 2020. A Comprehensive Survey on VANET Broadcast Protocols. In *2020 International Conference on Computation, Automation and Knowledge Management (ICCAKM)*, 298–302.

Jiang, J.; Dun, C.; Huang, T.; and Lu, Z. 2020. Graph Convolutional Reinforcement Learning. In *International Conference on Learning Representations*.

Jiang, J.; and Lu, Z. 2018. Learning Attentional Communication for Multi-Agent Cooperation. In *Proceedings of the 32nd International Conference on Neural Information Processing Systems*, NIPS’18, 7265–7275. Red Hook, NY, USA: Curran Associates Inc.

Kaviani, S.; Ryu, B.; Ahmed, E.; Kim, D.; Kim, J.; Spiker, C.; and Harnden, B. 2023. DeepMPR: Enhancing Opportunistic Routing in Wireless Networks through Multi-Agent Deep Reinforcement Learning. arXiv:2306.09637.

Kaviani, S.; Ryu, B.; Ahmed, E.; Larson, K. A.; Le, A.; Yahja, A.; and Kim, J. H. 2021. DeepCQ+: Robust and Scalable Routing with Multi-Agent Deep Reinforcement Learning for Highly Dynamic Networks. In *2021 IEEE Military Communications Conference, MILCOM 2021, San Diego, CA, USA, November 29 - Dec. 2, 2021*, 31–36. IEEE.

Kipf, T. N.; and Welling, M. 2017. Semi-Supervised Classification with Graph Convolutional Networks. In *International Conference on Learning Representations*.

Ma, X.; Zhang, J.; Yin, X.; and Trivedi, K. S. 2012. Design and Analysis of a Robust Broadcast Scheme for VANET Safety-Related Services. *IEEE Transactions on Vehicular Technology*, 61(1): 46–61.

Peng, P.; Wen, Y.; Yang, Y.; Yuan, Q.; Tang, Z.; Long, H.; and Wang, J. 2017. Multiagent Bidirectionally-Coordinated Nets: Emergence of Human-level Coordination in Learning to Play StarCraft Combat Games. arXiv:1703.10069.

Puterman, M. L. 1994. *Markov Decision Processes: Discrete Stochastic Dynamic Programming*. USA: John Wiley & Sons, Inc., 1st edition. ISBN 0471619779.

Qayyum, A.; Viennot, L.; and Laouiti, A. 2002. Multipoint relaying for flooding broadcast messages in mobile wireless networks. In *Proceedings of the 35th Annual Hawaii International Conference on System Sciences*, 3866–3875.

Riley, G. F.; and Henderson, T. R. 2010. *The ns-3 Network Simulator*, 15–34. Berlin, Heidelberg: Springer Berlin Heidelberg. ISBN 978-3-642-12331-3.

Scarselli, F.; Gori, M.; Tsoli, A. C.; Hagenbuchner, M.; and Monfardini, G. 2009. The Graph Neural Network Model. *IEEE Transactions on Neural Networks*, 20(1): 61–80.

Schulman, J.; Wolski, F.; Dhariwal, P.; Radford, A.; and Klimov, O. 2017. Proximal Policy Optimization Algorithms. arXiv:1707.06347.

Sukhbaatar, S.; Szlam, A.; and Fergus, R. 2016. Learning Multiagent Communication with Backpropagation. In *Proceedings of the 30th International Conference on Neural Information Processing Systems*, NIPS'16, 2252–2260. Red Hook, NY, USA: Curran Associates Inc. ISBN 9781510838819.

Suri, N.; Bredy, M.; Campioni, L.; Nilsson, J.; Cramer, E.; Fronteddu, R.; and Tortonesi, M. 2022. Comparing Performance of Group Communications Protocols Over SCB versus Routed MANET Networks. In *MILCOM 2022 - 2022 IEEE Military Communications Conference (MILCOM)*, 1011–1017.

Sutton, R. S.; and Barto, A. G. 2018. *Reinforcement Learning: An Introduction*. Cambridge, MA, USA: A Bradford Book. ISBN 0262039249.

Terry, J.; Black, B.; Grammel, N.; Jayakumar, M.; Hari, A.; Sullivan, R.; Santos, L. S.; Dieffendahl, C.; Horsch, C.; Perez-Vicente, R.; et al. 2021. Pettingzoo: Gym for multi-agent reinforcement learning. *Advances in Neural Information Processing Systems*, 34: 15032–15043.

Tonguz, O.; Wisitpongphan, N.; Bai, F.; Mudalige, P.; and Sadekar, V. 2007. Broadcasting in VANET. In *2007 Mobile Networking for Vehicular Environments*, 7–12.

Veličković, P.; Cucurull, G.; Casanova, A.; Romero, A.; Liò, P.; and Bengio, Y. 2018. Graph Attention Networks. In *International Conference on Learning Representations*.

Wang, Z.; Schaul, T.; Hessel, M.; Van Hasselt, H.; Lanctot, M.; and De Freitas, N. 2016. Dueling Network Architectures for Deep Reinforcement Learning. In *Proceedings of the 33rd International Conference on International Conference on Machine Learning - Volume 48*, ICML'16, 1995–2003. JMLR.org.

Weng, J.; Chen, H.; Yan, D.; You, K.; Duburcq, A.; Zhang, M.; Su, Y.; Su, H.; and Zhu, J. 2022. Tianshou: A Highly Modularized Deep Reinforcement Learning Library. *Journal of Machine Learning Research*, 23(267): 1–6.

Yahja, A.; Kaviani, S.; Ryu, B.; Kim, J. H.; and Larson, K. A. 2022. DeepADMR: A Deep Learning based Anomaly Detection for MANET Routing. In *IEEE Military Communications Conference, MILCOM 2022, Rockville, MD, USA, November 28 - December 2, 2022*, 412–417. IEEE.

Ye, Z.; and Zhou, Q. 2021. Performance Evaluation Indicators of Space Dynamic Networks under Broadcast Mechanism. *Space: Science & Technology*, 2021.

Supplementary Materials

Pseudo-code of the MPR Selection algorithm (Adjih, Jacquet, and Viennot 2005)

Algorithm 1: MPR Selection Heuristic

Require: The set N of one-hop neighbors

Ensure: The MPR set

```

1: Initialize MPR set with all members of  $N$  with willingness
   equal to WILL_ALWAYS
2: for each node  $y \in N$  do
3:   Calculate  $D(y)$ 
4: end for
5: Select nodes in  $N$  which cover the poorly covered nodes
   in  $N2$ . Remove these nodes from  $N2$ .
6: while nodes exist in  $N2$  not covered by at least
   MPR_COVERAGE nodes in the MPR set do
7:   for each node in  $N$  do
8:     Calculate reachability: number of nodes in  $N2$ 
       not yet covered by at least MPR_COVERAGE nodes in the
       MPR set and are reachable through this 1-hop neighbor.
9:   end for
10:  Select as MPR the node with highest willingness
      among nodes in  $N$  with non-zero reachability.
11:  if multiple choices then
12:    Select node providing maximum reachability to
      nodes in  $N2$ .
13:    if multiple nodes provide same reachability then
14:      Select node as MPR with greater  $D(y)$ .
15:    end if
16:  end if
17:  Remove nodes from  $N2$  now covered by
      MPR_COVERAGE nodes in the MPR set.
18: end while

```

$D(y)$ is defined as the number of symmetric neighbors of node y , excluding all the members of N and excluding the node performing the computation. A poorly covered node is a node in $N2$ which is covered by less than MPR_COVERAGE nodes in N . Note that in our implementation every node has willingness set to WILL_ALWAYS and MPR_COVERAGE is set to 1 to ensure that the MPR heuristic's overhead is kept to the minimum.

Implementation Details and Hardware Involved

Implementation Details Our framework, which is written in Python and based on PyTorch, implements a customized extension of the Tianshou (Weng et al. 2022) framework. The MARL environment is defined following the Petting-Zoo (Terry et al. 2021) API. The GAT and global max pooling employ the implementation provided by PyTorch Geometric (Fey and Lenssen 2019). Training and testing graphs were generated with the aid of the NetworkX library.

The main components can be found in the graph_env/env folder. In particular, the environment dynamics are defined in graph_env/env/graph.py and graph_env/env/utils/core.py. Networks

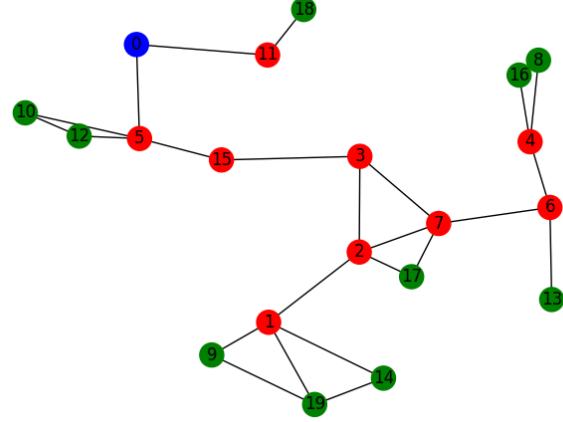


Figure 3: An example of visualized graph during testing, while employing L-DGN policies. Red nodes represent agents that have forwarded once. Green nodes represent agents that have received the message, but never forwarded it. Yellow (none) agents that haven't received the message yet. Purple (none) agents that have forwarded more than once. The blue node represents the source of the message.

and policy implementations can be found respectively in graph_env/env/utils/networks and graph_env/env/utils/policies.

Reproducing our results To ease testing and reproducibility, our framework comes with a Docker Image comprising all the necessary requirements that the reader can quickly build, allowing them to run the application in a containerized environment following the instructions listed below.

1) From the root project folder run the following command to build the image:

```
docker build -t marl_mpr .
```

1b) If the host machine does not have any GPU or if it is an Apple Mac device (including ones employing Apple M1 SoC) please use:

```
docker build -t marl_mpr \
```

```
-f Dockerfile.cpu .
```

2) Command example to run the container:

```
docker run --ipc=host --gpus all \
-v ${PWD}:/home/devuser/dev:Z \
-it --rm marl_mpr
```

Please note that --gpus all is optional and it should be omitted in case the hosting machine is not equipped with a GPU. Alternatively, the reader can also install the requirements needed in a dedicated Python (≥ 3.8) virtual environment by running

```
pip install -r requirements.txt
```

3) **Visualization (Optional).** A visualization aid is provided to watch the agents in action on the testing graphs (see Figure 3). If the Docker Image is used, the following two arguments should be added when running the container in order to render the figure: `-e DISPLAY=unix\$/DISPLAY` and `-v /tmp/.X11-unix:/tmp/.X11-unix`.³ The entire command to run the container while enabling visualization would be:

```
docker run --ipc=host --gpus all \
-e DISPLAY=unix$DISPLAY \
-v /tmp/.X11-unix:/tmp/.X11-unix \
-v ${PWD}:/home/devuser/dev:z \
-it --rm marl_mpr
```

Training models Trained models will be saved in the `log/algorithm_name/weights` folder as `model_name_last.pth`. Before the training process begins, the user will be asked if they want to log training data using the Weight and Biases (WANDB) logging tool.

- DGN-R

```
python train_dgn_r.py \
--model-name DGN-R
```

- L-DGN

```
python train_l_dgn.py \
--model-name L-DGN \
```

- HL-DGN

```
python train_hl_dgn.py \
--model-name HL-DGN
```

Seeding By default, the seed is set to 9. The reader can easily change such value using the argument `--seed X`, where X is the chosen seed. This seeding value is carefully set for `np_random.seed(X)`, `torch.manual_seed(X)`, `train_envs.seed(X)`, and `test_envs.seed(X)`. Other parameters can be changed from their default and they can be consulted via `python train_dgn_r.py --help`.

Testing models All three of our trained models, DGN-R, L-DGN, and LH-DGN, are found in their respective subfolders of the `/log` folder and results can be reproduced with the following command:

- DGN-R

```
python train_dgn_r.py --watch \
--model-name DGN-R.pth
```

³Please note that these arguments are valid only for machines running a Unix OS. Machines running MacOS might require installing a display server like XQuartz.

- L-DGN

```
python train_l_dgn.py --watch \
--model-name L-DGN.pth
```

- HL-DGN

```
python train_hl_dgn.py --watch \
--model-name HL-DGN.pth
```

- MPR Heuristic. In order to test MPR heuristic results add the boolean argument `--mpr-policy`. For example:

```
python train_hl_dgn.py --watch \
--model-name HL-DGN.pth \
--mpr-policy
```

Hardware Involved Our policies were trained using 40 parallel environments, on a workstation running Ubuntu 22.04 LTS, CUDA Toolkit v11.7 and equipped with an Intel i9-13900F CPU, 32GB DDR4 RAM, and an NVIDIA GeForce RTX 4090 GPU.

Topologies Dataset As mentioned in the Experiments Section, we have randomly generated two datasets containing connected graph topologies. The first has 20 nodes per graph, while the second has 50 nodes. Training and testing sets for each of the two sets contain, respectively, 50K and 100 graphs. The sole dataset takes up to 140MB compressed in a ZIP file with maximum compression level, for such a reason, and for reviewing purposes, we upload (along with the code) a reduced training set of topologies with 2500 graphs for each set (20 and 50). The testing sets are left unchanged for different numbers of agents (20/50) and the desired set can be changed with the `--n-agents` argument, which default value is set to 20. All the topologies can be found in the `/graph_topologies` folder.

Training Performance

Figure 4 presents the performance of our proposed methods, L-DGN and HL-DGN, when compared to the DGN-R baseline used, during the training process. We measure such performance in terms of the summation of the returns of each agent during the dissemination task across the entire graph, named "graph return". The reason is twofold: first, we use such metric to understand if the local rewards assigned to each agent correlate with a desired factorization of a centralized policy, measured in terms of summations of such rewards; furthermore, as our environment is highly dynamic in terms of the entities that contribute in the dissemination task at each timestep the summation of the returns reveals to be a more suitable metric rather than a more traditional average of the returns for each agent involved.

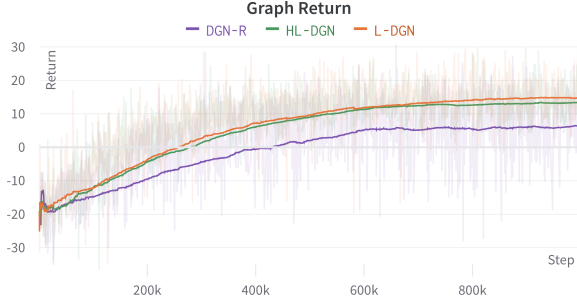


Figure 4: Summation of the returns received by every agent for each graph during training.

Ablation Study

Figure 5 and Figure 6 show the impact of the main components of our proposed L-DGN and HL-DGN. Similarly to what we introduced in Training Performance, Figure 5 illustrates the graph return metric during training. Figure 6, instead, shows an alternative global metric to assist the interpretation of the results, that is given by $\frac{\text{Coverage}^2}{\text{Messages}}$. Here the *Coverage* is the fraction of nodes that have received the message in the entire graph and *Messages* refers to the number of forwards recorded by all the agents employed in a graph.

Both figures depict six different methods during their training process. Two of them are the methods presented in the paper (L-DGN and HL-DGN) and one is our MARL baseline (DGN-R). The remaining three are ablations of our proposed L-DGN and HL-DGN architectures, namely DGN-R-Duel, L-DGN-MP, and L-DGN-MPNC:

DGN-R-Duel The implementation of this method lies in between L-DGN and DGN-R. Starting from the latter, we added the dueling network instead of a single MLP stream as the action decoder. Both figures show the positive impact of the dueling network in the final strategy, which significantly outperforms DGN-R after 600K steps. From such a learning trajectory, we can also deduce the impact of another main component of our L-DGN, the Local Horizon TD estimation (see Local Horizon and n-step TD Estimation). With the addition of such n-step estimation, we obtain our L-DGN architecture, and we can notice how such a component helps the learned strategy to converge earlier and less abruptly.

L-DGN-MP This method removes the second GAT layer of L-DGN and replaces it with the global max pool operator (later adopted by HL-DGN). The concatenation of the output of every encoding stage is still present here. We can notice a slight drop in performance when compared to L-DGN.

L-DGN-MPNC This method removes both the second GAT layer of L-DGN, as well as the concatenation of the output of every encoding stage. We notice a significant decrease in performance when compared to L-DGN. It can also be seen that HL-DGN can be derived from L-DGN-MPNC after the ablation of the MLP encoding stage and that HL-DGN does not suffer from such performance reduction.

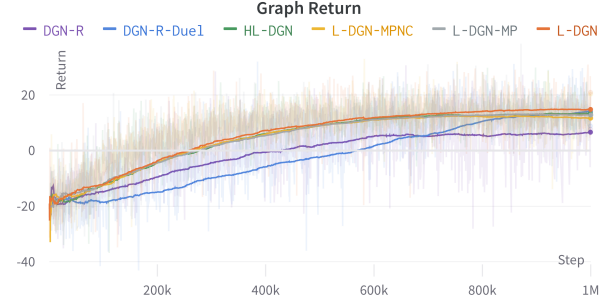


Figure 5: Graph return of the various methods used for the ablation study.

In summary, these ablation studies, centered around L-DGN allowed us to both understand the strengths of this approach when compared to DGN-R, as well as design our second proposed architecture (HL-DGN), which exhibits a simplified architecture, requires less communication overhead, and only slightly underperforms in terms of graph return during training.



Figure 6: Alternative global metric used to evaluate the learned strategies during the ablation study.

Hyperparameters

	Hyperparameter	Value
Training	Training steps	1×10^6
	Learning rate	1×10^{-3}
	Buffer size	1×10^5
	Gamma	0.99
	Batch size	32
	Exploration Decay	Exponential
	Local Horizon	4
	N-Step Estimation	4
	Training Frequency	1 every 10 steps
	Gradient Steps	1
	Parallel Training Envs	40
	Experience Replay	Uniform
Policy Parameters	Seed	9
	MLP Hidden Size	512
	GAT Attention Heads	4
	GAT Hidden Size	128 (each head)
	A-Network Hidden Sizes	[128, 128]
	V-Network Hidden Sizes	[128, 128]

Table 3: Hyperparameters used across our experiments. "Uniform" indicates that no prioritized replay has been used and experiences where uniformly sampled.